

Contents lists available at [ScienceDirect](http://ScienceDirect.com)

## Matrix Biology

journal homepage: [www.elsevier.com/locate/matbio](http://www.elsevier.com/locate/matbio)

## Quantitative proteomics at different depths in human articular cartilage reveals unique patterns of protein distribution



Catharina Müller<sup>a,1,2</sup>, Areej Khabut<sup>b,2</sup>, Jayesh Dudhia<sup>c</sup>, Finn P. Reinholt<sup>d</sup>, Anders Aspberg<sup>a</sup>, Dick Heinegård<sup>b,3</sup>, Patrik Önnerfjord<sup>b,\*</sup>

<sup>a</sup> Department of Biology, University of Copenhagen, Biocenter, DK-2200 Copenhagen N, Denmark

<sup>b</sup> Department of Clinical Sciences Lund, Lund University, BMC-C12, 221 84 Lund, Sweden

<sup>c</sup> Department of Clinical Sciences and Services, The Royal Veterinary College, University of London, Hatfield, United Kingdom

<sup>d</sup> Department of Pathology, University of Oslo and Oslo University Hospital, Rikshospitalet, Oslo, Norway

### ARTICLE INFO

#### Article history:

Received 11 June 2014

Received in revised form 20 August 2014

Accepted 22 August 2014

Available online 1 September 2014

#### Keywords:

Articular cartilage

Cartilage biology

Extracellular matrix proteins

Proteomics

Proteoglycan

Multiple reaction monitoring

### ABSTRACT

The articular cartilage of synovial joints ensures friction-free mobility and attenuates mechanical impact on the joint during movement. These functions are mediated by the complex network of extracellular molecules characteristic for articular cartilage. Zonal differences in the extracellular matrix (ECM) are well recognized. However, knowledge about the precise molecular composition in the different zones remains limited. In the present study, we investigated the distribution of ECM molecules along the surface-to-bone axis, using quantitative non-targeted as well as targeted proteomics.

In a discovery approach, iTRAQ mass spectrometry was used to identify all extractable ECM proteins in the different layers of a human lateral tibial plateau full thickness cartilage sample. A targeted MRM mass spectrometry approach was then applied to verify these findings and to extend the analysis to four medial tibial plateau samples.

In the lateral tibial plateau sample, the unique distribution patterns of 70 ECM proteins were identified, revealing groups of proteins with a preferential distribution to the superficial, intermediate or deep regions of articular cartilage. The detailed analysis of selected 29 proteins confirmed these findings and revealed similar distribution patterns in the four medial tibial plateau samples.

The results of this study allow, for the first time, an overview of the zonal distribution of a broad range of cartilage ECM proteins and open up further investigations of the functional roles of matrix proteins in the different zones of articular cartilage in health and disease.

© 2014 Published by Elsevier B.V. This is an open access article under the CC BY-NC-ND license (<http://creativecommons.org/licenses/by-nc-nd/3.0/>).

### 1. Introduction

Articular cartilage is a highly specialized tissue that serves to facilitate joint mobility and to withstand mechanical load on the joint (Buckwalter and Mankin, 1998; Bhosale and Richardson, 2008). Its extensive ECM has a unique composition to meet the specific needs of the tissue (Mow et al., 1992). It consists mainly of collagens and heavily

charged proteoglycans. A variety of non-collagenous matrix proteins add to the complexity and is important for ECM assembly and tissue maintenance (Heinegård, 2009; Schaefer and Schaefer, 2010).

The articular cartilage matrix is organized differently depending on the distance from the chondrocyte but also depending on the depth from the articular surface (Buckwalter and Mankin, 1998; Guilak et al., 2006; Bhosale and Richardson, 2008; Mittelstaedt et al., 2011). Four zones are distinguished morphologically from the articular cartilage surface to the cartilage–bone interface (Kato et al., 1988; Buckwalter and Mankin, 1998; Hunziker et al., 2002; Bhosale and Richardson, 2008; Fig. 1). The thin superficial zone is characterized by flattened ellipsoid cells and thin collagen fibrils arranged parallel to the surface, providing shear and tensile strength. The intermediate zone contains spheroid-shaped cells and randomly arranged fibres. The deep zone is rich in glycosaminoglycans and shows spheroid-shaped chondrocytes, which are arranged in columns perpendicular to the surface (Youn et al., 2006). The zone of calcified cartilage connects to the subchondral bone (Redler et al., 1975; Hoemann et al., 2012).

**Abbreviations:** ECM, extracellular matrix; iTRAQ, isobaric tags for relative and absolute quantification; LTP, lateral tibial plateau; MS, mass spectrometry; MTP, medial tibial plateau; MRM, multiple reaction monitoring.

\* Corresponding author at: Department of Clinical Sciences Lund, Section of Rheumatology, BMC-C12, Lund University, SE-22184 Lund, Sweden. Tel.: +46 46 2223129; fax: +46 46 2113417.

E-mail addresses: [catharina.muller@med.lu.se](mailto:catharina.muller@med.lu.se) (C. Müller),

[patrik.onnerfjord@med.lu.se](mailto:patrik.onnerfjord@med.lu.se) (P. Önnerfjord).

<sup>1</sup> Present address: Department of Experimental Medical Science, Lund University, BMC-D12, 221 84 Lund, Sweden.

<sup>2</sup> Catharina Müller and Areej Khabut contributed equally to this work.

<sup>3</sup> Deceased.

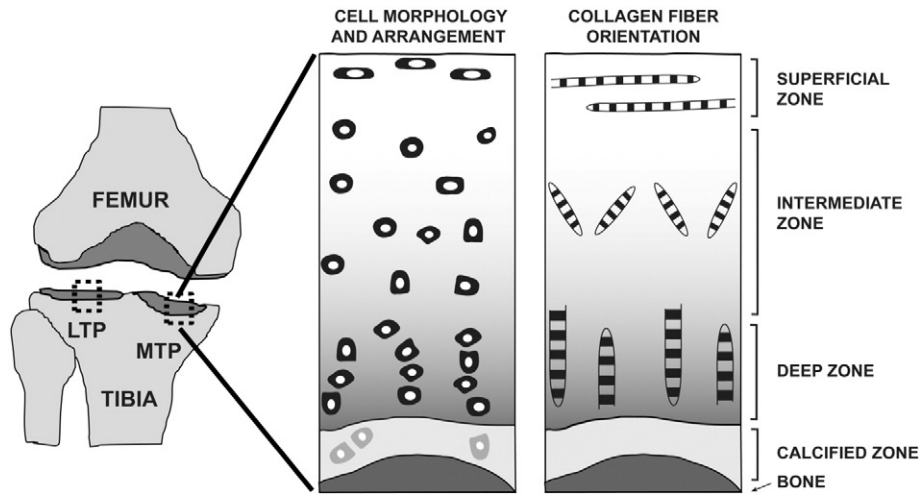


**Fig. 1.** Articular cartilage zones. Four zones can be distinguished morphologically in articular cartilage. The boxes represent the sample plugs taken from the lateral tibial plateau (LTP) and the medial tibial plateau (MTP). The insert illustrates the cell distribution and the collagen fibril orientation across the full thickness cartilage.

Events that lead to changes in this intricate organization may lead to the development of pathological conditions (Heinegård, 2009). Mechanical injury or disturbances of tissue maintenance, as for example in osteoarthritis, may trigger cells to alter the ECM structure and thus impair the mechanical strength of the tissue (Hunziker, 2002). To understand pathological processes and allow more accurate diagnosis and tailor-made therapy of joint diseases, it is important to know the molecular composition of the tissues involved, including variations between the different zones of the cartilage.

In the past, several studies have been undertaken to characterize these zones with regard to structural organization (Hunziker et al., 2002; Schumacher et al., 2002; Youn et al., 2006), and protein localisation (Schumacher et al., 1994; DiCesare et al., 1995; Lorenzo et al., 1998a; Pfister et al., 2001; Söder et al., 2002; Veje et al., 2003). Generally, these studies focused on one or two components, due to technical restrictions, and could therefore not provide a broad overview. Recently, genomic (Fukui et al., 2008; Grogan et al., 2013) and proteomic studies (Zhang et al., 2011; Cillero-Pastor et al., 2013) were applied to investigate gene expression and protein distribution patterns with a broader scope. Challenges with articular cartilage proteomics include the scarce availability of healthy human articular cartilage biopsies, the high degree of cross-linking between the ECM molecules, and the difficulty in identifying low abundant proteins, particularly in the presence of highly abundant proteins and proteoglycans such as collagens and aggrecan.

The aim of the present study was to quantitatively analyze extractable proteins in human articular cartilage to provide a detailed overview of the protein distribution. This was achieved by first applying a non-targeted mass spectrometry approach (iTRAQ technology) and subsequently by analyzing protein distribution in detail using a targeted approach (MRM technology; Fig. 2).

We found unique patterns of protein distribution throughout the different zones of the articular cartilage. This detailed characterization strengthens our understanding of articular cartilage matrix composition and forms the basis for further investigations of key molecules in tissue function, maintenance and pathology.

## 2. Results

### 2.1. Quantitative mass spectrometry—discovery approach

To test the feasibility of the study and to get an overview about the extractable ECM proteins in articular cartilage, iTRAQ labeled protein mixtures of the different depth zones of a LTP sample were analyzed using Q-TOF tandem mass spectrometry. This discovery approach

allowed the quantification of 277 proteins. The total protein list, including the weighted average protein ratio (versus reference sample) for each sample pool (pools 1–9) is presented in Supplementary Table S1. Each iTRAQ set was run individually and analyzed separately by calculating the sample-to-reference ratio. The number of peptide ratio measurements for each identified protein varied from  $n = 1$  (in a few instances listed in italics in Table 1 and Supplementary Table S1) to approximately 100 for, e.g. collagen and fibronectin. To focus the analysis on cartilage ECM proteins, a subset of 70 proteins was selected (Table 1). Plasma proteins, membrane proteins and intracellular proteins were excluded (Supplementary Table S2). Additionally, collagens except collagen type VI were removed from the list. Due to the high degree of cross-linking in collagens, except collagen type VI, these molecules are poorly extracted and cannot be quantitatively analyzed. Different distribution patterns of ECM proteins in the LTP sample were found (Fig. 3). Several proteins showed a distinct preference for the superficial region, e.g. asporin, tenascin-C and collagen type VI (Fig. 3a). Others were found to be more abundant with increasing depth, e.g. aggrecan (G1, G2 and G3 domains), hyaluronan and proteoglycan link protein 1 (link protein) and chondroadherin (Fig. 3c). Some showed an even distribution throughout the tissue, e.g. decorin and PRELP (Fig. 3d). Only thrombospondin-1 and mimecan were found to be enriched in the middle region (Fig. 3b).

### 2.2. Data verification using MRM mass spectrometry

From the 70 cartilage ECM proteins identified by the iTRAQ approach, 29 proteins of special interest in articular cartilage were selected for analysis by the MRM technology (marked in Table 1). The advantage of the MRM approach is that pre-optimized assays for selected, unique peptides are used, which provides higher sensitivity. Furthermore, we were able to measure the proteins using a single chromatography step without prior ion-exchange chromatography enabling us to instead take more data points across the cartilage depth, thereby achieving enhanced detail in the protein distribution patterns.

Quantitative analysis of the protein distribution in the LTP sample via iTRAQ and MRM approaches resulted in similar protein distribution patterns for all analyzed proteins (Fig. 3). After having established the feasibility of the study, the MRM approach was now used for a detailed analysis of protein distribution patterns in four MTP samples. The MRM transition list and the quantitative data for each peptide, allowing the quantification of the respective protein in the LTP and the four MTP samples, are shown in Supplementary Table S3 and S4a-e.

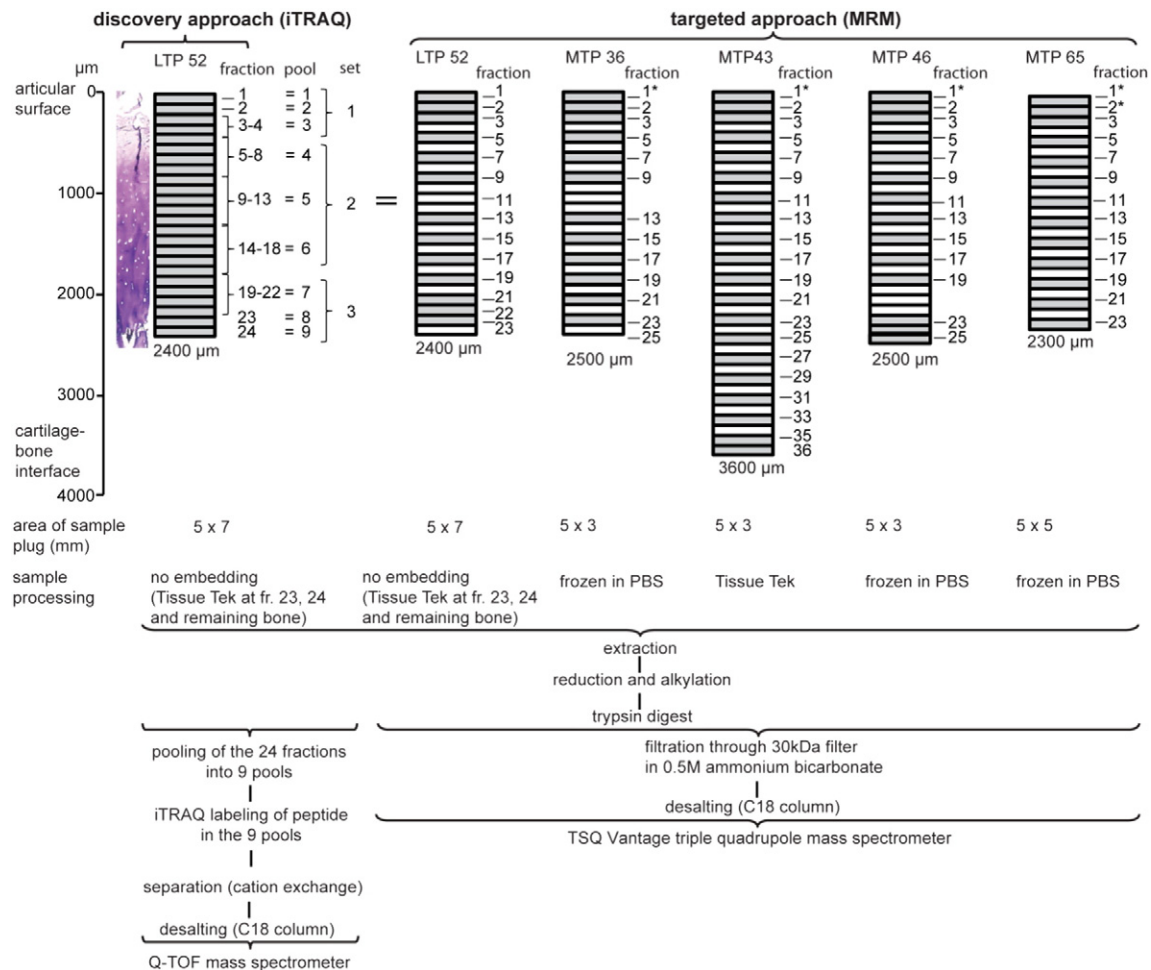


**Fig. 2.** Overview of the samples and sample preparation. Schematic depiction of the sample plugs and the collected tissue fractions (each fraction containing 10 sections of 10  $\mu\text{m}$  each) collected by cryosectioning beginning at the articular surface. Grey boxes represent tissue extracts used for mass spectrometry analysis. To test the feasibility of the study, extracts from the same lateral tibial plateau (LTP) sample were quantitatively analyzed using the iTRAQ labeling technology and the label-free MRM approach. Next, the MRM approach was used to identify protein distribution patterns in four different medial tibial plateau (MTP) samples. A Toluidine blue-stained tissue section (cross-section) from a sample adjacent to the one used for vertical sectioning of LTP52 is shown. Note the gradient in staining indicating differences in proteoglycan content. \*, Sections which did not represent full area of the sample plug due to technical difficulties, actual protein content might be underrepresented.

### 2.3. Protein distribution patterns in four MTP samples

In the four MTP samples (MTP36, MTP43, MTP46 and MTP65), protein distribution patterns similar to the ones identified in the LTP sample were found. For most proteins, the protein distribution pattern of a given protein was similar in the four MTP samples. For a limited number of proteins (fibronectin, versican, COMP and biglycan), no consistent pattern could be established (Fig. 6g; Supplementary Table S4a-e).

#### 2.3.1. Proteins in the superficial region

Proteins identified with a preferential distribution in the superficial region of the samples were asporin, tenascin-C, thrombospondin-4 and perlecan (Fig. 4a) as well as dermatopontin, collagen alpha-1 (VI) and collagen alpha-3 (VI; Supplementary Table S4a-e). These proteins showed peak abundance within the uppermost 20% of the total tissue depth (Table 2 and Supplementary Table S5). Below the zone of maximum abundance, the protein content decreased rapidly towards the deeper regions.

#### 2.3.2. Proteins in the deep region

Aggrecan G1 domain (as well as the G2 and G3 domains), link protein, chondroadherin and osteoadherin showed a marked increase

of protein content towards the deep region of the samples (Fig. 4b). Further examples are matrix Gla protein, matrilin-3, osteonectin (SPARC) and serin protease HTRA1 (Supplementary Table S4a-e). These proteins showed highest abundance between 60% and 100% of the tissue depth, often in the deepest layers (Table 2 and Supplementary Table S5). An exception is aggrecan G1 domain in the MTP65 sample, which peaked at a depth of 850  $\mu\text{m}$  and then remained at an even level throughout the deeper tissue. Interestingly, MTP43 stands in sharp contrast to the other MTP samples since the abundance of several proteins was found to decrease towards the deepest layers after a peak at 60%–80% of the tissue depth.

#### 2.3.3. Proteins in the intermediate region

Only mimecan and thrombospondin-1 were found to be enriched in the middle part of the MTP samples (Fig. 5a). They showed highest abundance between 20% and 35% of tissue depth (Table 2). These proteins decreased towards the deeper layer, but not as much as the predominantly superficial proteins.

#### 2.3.4. Evenly distributed proteins

Lumican, fibromodulin, decorin and PRELP showed an even distribution throughout the tissue (Fig. 5b). However, they seemed to be less abundant in the most superficial layers.

**Table 1**

Filtered list on quantitative proteomics data of the LTP52 sample (iTRAQ).

The average ratios versus the reference sample are listed. The accession numbers are derived from the SwissProt database. The complete list of identified proteins is available in Supplementary Table S1. Single peptide quantifications are shown in italics. Empty cells indicate no identification. Proteins marked in (a) were also measured via MRM mass spectrometry.

Protein name	Accession	(a)	Pool 1	Pool 2	Pool 3	Pool 4	Pool 5	Pool 6	Pool 7	Pool 8	Pool 9
Aggrecan core protein	P16112		0.11	0.12	0.23	0.27	0.42	0.64	1.24	0.89	1.76
Aggrecan G1 domain	P16112	X	0.120	0.118	0.247	0.263	0.404	0.607	1.291	0.983	1.969
Aggrecan G2 domain	P16112	X	0.057	0.085	0.148	0.289	0.449	0.677	1.215	0.787	1.484
Aggrecan G3 domain	P16112	X	0.132	0.165	0.218	0.230	0.330	0.528	0.783	0.472	0.888
Alpha-1-antichymotrypsin	P01011		2.30	2.20	3.70	0.96	0.19	0.08			
Alpha-1-antitrypsin	P01009		2.76	2.53	3.52	0.65	0.12	0.09	0.08	0.05	0.15
Angiogenin	P03950		0.19	0.35	0.42	0.23	0.41	1.13	7.71	6.46	15.74
Apolipoprotein A-I	P02647		5.08	4.00	4.96	1.00	0.30	0.24	0.16	0.15	0.46
Apolipoprotein D	P05090		0.18	0.16	0.19	0.09	0.11	0.37			
Asporin	Q9BXN1	X	1.90	1.78	1.34	0.17	0.03	0.01	0.03	0.01	0.04
Biglycan	P21810	X	0.39	0.54	0.89	0.49	0.43	0.50	0.66	0.39	0.75
Cartilage intermediate layer protein 1-1	O75339	X	0.05	0.04	0.03	0.04	0.04	0.04	0.23	0.24	0.50
Cartilage intermediate layer protein 1-2	O75339b	X	0.12	0.14	0.12	0.09	0.16	0.26	0.53	0.40	0.85
Cartilage intermediate layer protein 2-1	Q8IUL8	x	0.19	0.02	0.08	0.07	0.01	0.19	0.24	0.14	0.45
Cartilage intermediate layer protein 2-2	Q8IUL8b	X	0.15	0.19	0.34	0.22	0.19	0.22	0.27	0.19	0.35
Cartilage oligomeric matrix protein (COMP)	P49747	X	0.51	0.49	0.61	0.27	0.31	0.44	0.79	0.58	1.12
Chondroadherin	O15335	X	0.03	0.02	0.03	0.02	0.04	0.12	0.37	0.32	0.67
Clusterin	P10909		0.28	0.25	0.38				0.92	0.52	0.99
Collagen alpha-1 (VI) chain	P12109	X	1.11	0.59	0.63	0.19	0.08	0.05	0.08	0.07	0.10
Collagen alpha-2 (VI) chain	P12110		0.97	0.47	0.49	0.17	0.08	0.06	0.06	0.04	0.08
Collagen alpha-3 (VI) chain	P12111	x	0.98	0.48	0.51	0.14	0.06	0.05	0.08	0.05	0.09
Collagen (II) chondrocalcin	P02458c		0.22	0.21	0.30	0.03	0.06	0.10	0.15	0.09	0.17
Collagen (II) N-propep	P02458					0.10	0.09	0.15			
C-type lectin domain family member 11A	Q9Y240					0.27	0.40	0.32	0.00	0.19	0.17
C-type lectin domain family member 3A	O75596		0.03	0.04		0.01	0.02	0.01	0.07	0.06	0.12
Decorin	P07585	x	0.56	0.62	0.85	0.43	0.35	0.38	0.56	0.38	0.81
Dermatopontin	Q07507	x	0.49	0.58	0.51	0.03	0.01	0.00	0.03	0.03	0.06
EGF-like repeat and discoidin 1-like domain-containing p.3	O43854		0.28	0.30	0.47	0.38	0.38	0.40			
Extracellular superoxide dismutase [Cu-Zn]	P08294		0.51	0.63	0.91	0.29	0.13	0.10	0.09	0.10	0.17
Fibroblast growth factor-binding protein 2	Q09BYJ		0.00	0.00	0.00	0.09	0.12	0.40	1.18	0.72	1.76
Fibromodulin	Q06828	x	0.08	0.15	0.31	0.23	0.31	0.39	0.68	0.41	0.79
Fibronectin	P02751	x	0.24	0.15	0.12	0.04	0.05	0.05	0.21	0.21	0.41
Fibulin-1	P23142		3.29	0.99	0.72						
Galectin-1	P09382		0.66	0.60	0.53	0.27	0.30	0.29			
Galectin-3	P17931								0.00	0.20	0.20
Hyaluronan and proteoglycan link protein 1 (link protein)	P10915	x	0.04	0.06	0.16	0.24	0.28	0.40	0.61	0.30	0.64
Interalpha-trypsin inhibitor heavy chain H1	P19827		4.28	2.41	1.72						
Lactadherin	Q08431		0.10	0.10	0.15	0.10	0.08	0.12	0.22	0.14	0.29
Leukocyte cell-derived chemotaxin-2	O14960		0.11	0.09	0.17	0.07	0.14	0.50	1.53	1.04	2.37
Lubricin (Proteoglycan 4)	Q92954	x	0.60	0.26	0.17	0.04	0.02	0.03	0.03	0.02	0.06
Lumican	P51884	x	0.54	0.74	1.00	0.49	0.30	0.19	0.22	0.12	0.25
Lysozyme C	P61626		0.06	0.03	0.04	0.07	0.10	0.29	1.38	1.43	3.56
Matrilin-1	P21941		0.07	0.07	0.08	0.01	0.02	0.02	0.02	0.02	0.05
Matrilin-3	O15232	x	0.12	0.01	0.05	0.07	0.24	0.44	0.60	0.21	0.32
Matrix Gla protein	P08493	x				0.00	0.10	0.05	0.49	1.02	1.86
Metalloproteinase inhibitor 3	P35625		0.02	0.12	0.13	0.00	0.11	0.18	1.00	0.58	1.48
Mimecan	P20774	x	0.75	1.03	1.52	0.85	0.58	0.36	0.19	0.07	0.13
Osteoadherin (Osteomodulin)	Q99983	x				0.03	0.12	0.19			
Osteonectin (SPARC)	P09486	x	0.07	0.22	0.19				0.28	0.31	1.75
Osteopontin	P10451	x							0.29	13.72	21.10
Perlecan	P98160	x	0.82	0.54	0.37	0.07	0.01	0.07	0.00	0.06	0.13
Phospholipase A2, membrane associated	P14555		0.11	0.11	0.15	0.44	1.24	6.33	6.33	8.46	21.1
Pleckstrin homology domain-containing family A6	Q9Y2H5								6.59	6.52	15.24
Procollagen C-endopeptidase enhancer 1	Q15113		2.70	2.01	4.67	1.46	1.45	1.14			
Procollagen C-endopeptidase enhancer 2	Q9UKZ9		0.22	0.25	0.33	0.24	0.28	0.36	0.55	0.32	0.72
PRELP	P51888	x	0.26	0.35	0.54	0.41	0.38	0.41	0.54	0.31	0.61
Protein S100-A9	P06702		0.31	0.22	0.36				0.19	0.33	1.26
Retinoic acid receptor responder protein 2	Q99969		0.01	0.43	0.57	0.56	1.05	1.68	3.34	2.51	6.34
Secreted frizzled-related protein 3	Q92765		0.23	0.25	0.42	0.22	0.25	0.24	0.61	0.33	0.81
Serine protease HTRA1	Q92743	x	0.81	0.47	0.38	0.14	0.11	0.19	0.50	0.34	0.69
SPARC-related modular calcium-binding protein 2	Q9H3U7		0.00	0.09	0.18	0.17	0.11	0.26	0.54	0.38	0.95
Stromelysin-1	P08254		8.01	7.21	11.28	3.89	1.30	0.67	0.41	0.10	0.38
Sushi repeat-containing protein SRPX2	O60687		0.27	0.44	0.43	0.16	0.15	0.12	0.25	0.16	0.30
Target of Nesh-SH3	Q7Z7G0		0.37	0.41	0.44	0.11	0.05	0.03	0.03	0.01	0.03
Tenascin-C	P24821	x	3.23	2.42	1.49	0.25	0.05	0.02			
Tenascin-X	P22105		0.83	0.70	0.59	0.12	0.07	0.15	0.21	0.00	0.06
Tetranectin	P05452		1.08	1.16	1.64	0.68	0.51	0.13	0.09	0.01	0.08
Thrombospondin-1	P07996	x	0.14	0.21	0.44	0.48	0.44	0.38	0.30	0.14	0.26
Thrombospondin-3	P49476		0.25	0.25	0.29						
Thrombospondin-4	P35443	x	0.26	0.25	0.29	0.00	0.00	0.00	0.18	0.02	0.22
TGF-beta-induced protein ig-h3	Q15582		1.27	0.70	0.66	0.17	0.05	0.05	0.00	0.01	0.15

(continued on next page)

**Table 1** (continued)

Protein name	Accession	(a)	Pool 1	Pool 2	Pool 3	Pool 4	Pool 5	Pool 6	Pool 7	Pool 8	Pool 9
<i>TNF receptor superfamily member 11B</i>	O00300		<i>0.04</i>	<i>0.02</i>	0.06	0.08	<i>0.03</i>	<i>0.12</i>	<i>0.11</i>	<i>0.04</i>	<i>0.10</i>
<i>Versican</i>	P13611	x	0.18	0.09	0.08	<i>0.04</i>	0.05	0.06	0.11	0.07	0.12
<i>Vitronectin</i>	P04004		10.75	7.67	7.61	1.45	0.22	0.09			
<i>72 kDa type IV collagenase</i>	P08253		2.23	2.30	3.55						

The numbers in italics represent quantification data originating from a single peptide.

### 2.3.5. Outlining cartilage tissue boundaries in the samples

In an attempt to set the identified protein distribution patterns in the LTP and MTP samples into perspective, we analyzed the distribution pattern of the superficial zone protein lubricin (Schumacher et al., 1994), the bone protein osteopontin (Franzen and Heinegård, 1985; Sodek et al., 2000) and several serum proteins (Fig. 6). In the LTP52 sample, lubricin was found to be confined to the most superficial layer (Fig. 6a). Lubricin was also found in the superficial part of the MTP samples (Fig. 6b). However, it is interesting to note that the lubricin content showed a less pronounced decrease toward the deeper layers in MTP43 and MTP65. Osteopontin was most prominently detected in the deepest layers of the LTP52 sample (Fig. 6c) and the MTP samples (Fig. 6d). However, considering the absolute peak area instead of the normalized values, only very low levels of the protein could be detected in the MTP43 sample (Fig. 6e), indicating that we did not reach the calcified/mineralized zone for this sample. Similar patterns were observed for osteonectin (SPARC; Supplementary Table S4a–e). Serum proteins showed different penetrations into the tissue depending on the molecular size (Fig. 6f). The smaller ones, alpha-1-acid glycoprotein 1 and serum albumin, were found to be accumulated in a depth of 500 µm of the LTP52 sample but were less present in the deeper regions. The larger proteins, fibronectin and alpha-2-macroglobulin, were found at high concentrations in the uppermost layers and in the deepest layers. A bias in the analysis of protein distribution patterns is introduced if proteins are present in the serum infiltrating the cartilage as well as produced by chondrocytes, as in the case of fibronectin. Interestingly, the fibronectin distribution patterns differ between the different MTP samples (Fig. 6g).

## 3. Discussion

Using quantitative mass spectrometry, we established the distribution patterns of a broad range of ECM proteins in articular cartilage (Supplementary Fig. S1a). This resulted in the identification of groups of proteins being enriched in the superficial region in the uppermost 20% of total tissue depth, of proteins enriched in the intermediate region between 20% and 35 % of total tissue depth and proteins enriched between 60% and 100% of total tissue depth (Supplementary Fig. S1b).

These findings are in accordance with the long-established notion of articular cartilage being a composite of different zones with distinct molecular composition and functional roles. These roles include the maintenance of a tear-resistant and lubricating joint surface, a shock-absorbing and elastic matrix and a connection to the subchondral bone. We do not yet fully understand the complex networks of proteins required to achieve these tasks. A detailed mapping of molecular composition will form the basis for further studies on molecular interactions and functional properties of the different zones. In this study, we used the term region (superficial, intermediate and deep, respectively), to refer to proteins showing predominance in certain parts of the samples. Future studies correlating our findings with morphological criteria defining the established term cartilage zones will further increase the understanding of articular cartilage biology.

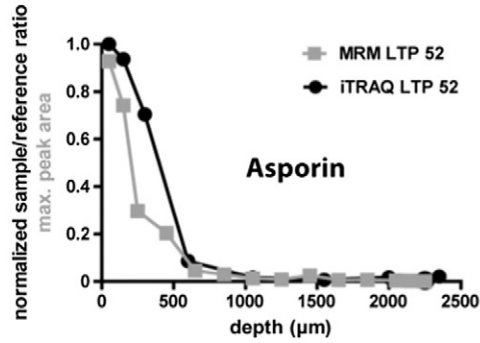
Our study of four human MTP samples revealed a subset of proteins with predominance in the superficial parts of the samples. Proteins such as asporin and tenascin-C showed strict confinement to the uppermost 20% of the samples (Fig. 4a; Table 2), while others such as perlecan and collagen type VI were also present in deeper zones albeit to a lesser

degree (Fig. 4a; Supplementary Tables S4a–e and S5). The presence of lubricin in the superficial zone has been established by several studies; it is known to be produced by superficial chondrocytes to lubricate the joint surface (Schumacher et al., 1994). The highest abundance of lubricin in the superficial part of the samples confirmed that the analyzed cartilage plugs had an intact joint surface and were sampled in a correct way. However, it is interesting to note that the lubricin abundance peaked in a region just below the most superficial layers in MTP 36, 43 and 46. It should be mentioned that the very first fraction of MTP36, 43 and 46 and the first two fractions of MTP65 contained protein extracts of slightly incomplete tissue sections due to technical difficulties in aligning the sample joint surface with the microtome knife (Fig. 2). The actual protein content may thus be slightly under-represented in these fractions. However, this does not explain why several superficial proteins showed peaks in protein abundance just underneath the most superficial layers since the lower levels of superficial region proteins were seen also in subsequent, complete sections. An interesting exception is the MTP65 sample, where these proteins were found to be highest in the most superficial layers, as was the case in the LTP52 sample. MTP65 was derived from the oldest donor, suggesting that the superficial zone could be abraded in the older samples. Differences in the protein distribution patterns could also indicate variation between the individual samples. One might also take these reflections into consideration for the proteins where no consistent distribution pattern could be established since the variation between the samples was too large (Supplementary Table S4a–e). However, the distribution patterns of asporin, tenascin-C and thrombospondin-4 are remarkably similar, which suggests a structural-functional relation of these proteins in the superficial region. In the future, these established techniques will be used to study age-related differences to elucidate possible changes in protein distribution during aging.

The other distinct subset identified in our study consists of proteins that are steadily increasing in abundance towards the deep part of the tissue, e.g. aggrecan, link protein, chondroadherin and osteoadherin (Fig. 4b; Supplementary Table S4a–e). Variations in proteoglycan and glycosaminoglycan distribution in articular cartilage are well established (Stockwell and Scott, 1967; Poole et al., 1982; Bayliss et al., 1983). Our data of increasing aggrecan with tissue depth, shown for all three domains G1, G2 and G3 in both the LTP and the MTP samples, fits well with these studies. Another important observation is that all the predominantly deep proteins showed an ultimate decrease towards the deepest layers in the MTP43 sample, in contrast to the other samples. However, it is interesting to note that the distribution patterns of MTP43 are in good agreement with the other samples down to 2200 µm.

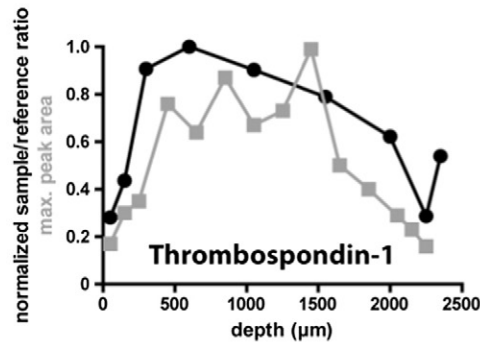
To delineate the sample boundaries, we analyzed the distribution pattern of the bone protein osteopontin (Fig. 6c,d). Osteopontin is detected in high abundance only in the deepest part of most samples (except for MTP43). This confirms that the deepest layers were reached in these samples, i.e. the calcified zone and possibly upper parts of the subchondral bone. Consequently, this means that no deep tissue areas are missing in MTP36, 46 and 65. However, for unknown reasons, we could only detect very low absolute levels of osteopontin in the much thicker cartilage sample MTP43 (Fig. 6e). We conclude from this that the deepest fractions contain proteins just from the beginning of the calcified zone or the bone tissue and therefore that the analyzed sample contains mainly cartilage tissue.

a) superficial



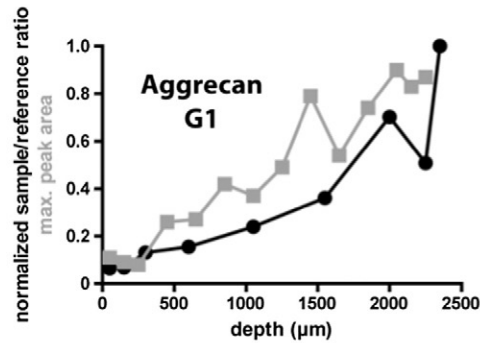
similar distribution pattern:  
Lubricin  
Tenascin-C  
Collagen type VI  
( $\alpha$ -1 / -2 / -3 chain)  
Dermatopontin  
Thrombospondin-4  
Perlecan

b) intermediate



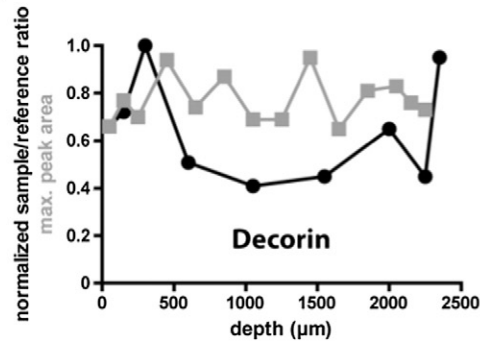
similar distribution pattern:  
Mimecan

c) deep



similar distribution pattern:  
Aggrecan G2, G3  
Link protein  
Chondroadherin  
Fibromodulin  
Matrix Gla protein  
Osteopontin  
Osteonectin (SPARC)

d) even



similar distribution pattern:  
PRELP  
COMP  
Biglycan

**Fig. 3.** Protein distribution patterns in the LTP sample. In a discovery approach using the iTRAQ technology, proteins with a preferential distribution to the superficial (a), intermediate (b) or deep (c) region of the LTP sample were identified. Some proteins showed even (d) distribution throughout the sample. This was verified by analyzing the same extract using the MRM approach. iTRAQ data (black circles) and MRM data (grey boxes) were normalized to 1 by division of each data point with the highest one for a given protein or peptide, respectively.

Thickness variation in the tibia cartilage has been reported, as well as correlation to the body weight and height of the donor (Ateshian et al., 1991; Shepherd and Seedhom, 1999; Li et al., 2005). Ateshian et al. investigated 12 human MTPs identifying a mean thickness of

$2.42 \pm 0.61$  mm (Ateshian et al., 1991). Our own experience (unpublished data) is that the thickness at any specified site does vary between individuals of similar age, although thinning with age is the general pattern.

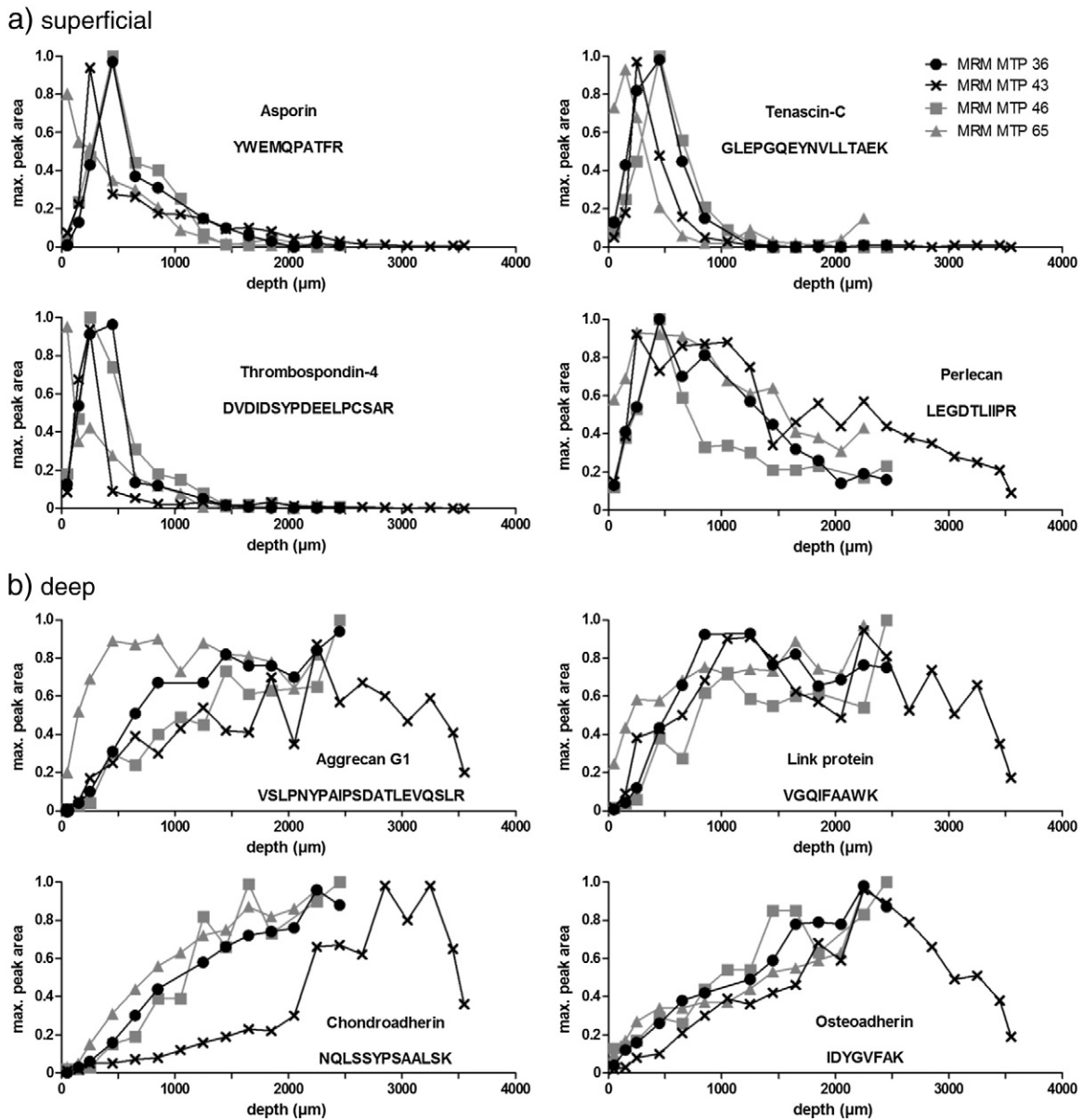


**Fig. 4.** Proteins enriched in the superficial or the deep region of the MTP samples. Proteins with a preferential distribution in the superficial (a) or in the deep (b) region of the MTP samples were quantified via MRM mass spectrometry. The peptide selected for the MRM assay is indicated for the respective protein. The MRM data were normalized to 1 by division of each data point with the highest one for a given peptide.

It is interesting to note that asporin and chondroadherin showed reversed distribution patterns throughout the tissue. The same contrary pattern was observed when comparing different cartilage tissues with each other (Önnerfjord et al., 2012). Asporin was found to be high in the fibrocartilage of the meniscus in comparison to articular cartilage, while chondroadherin was found to be low in the meniscus but highly abundant in various articular cartilages. The functional aspects of this observation are still unknown.

Some proteins, such as PRELP and decorin, were fairly evenly distributed (Fig. 5b). However, they seem to be absent from the most superficial layers, as observed for several proteins with predominance in the uppermost 20% of the tissue. This might indicate a thus far unknown complexity in a zone just underneath the most superficial layers, which may be related to recent observations of distinct biophysical properties in this region (Buckley et al., 2010). Interestingly, only mimecan and thrombospondin-1 showed predominance in the middle part of the MTP samples (Fig. 5a; Table 2). A hypothesis for explaining the scarcity of proteins with predominance in the intermediate zone

could be that this zone shares basic structural and functional roles with all zones in the articular cartilage. Consequently, the important proteins for these functions would be the ones with a broad or even distribution throughout the tissue, like the members of the small leucine-rich repeat proteins, and the bulk of the different collagens. Since these collagens are heavily cross-linked, they are not sufficiently extracted with the methodology used in this study, except for collagen type VI, and could not be analyzed. The cartilage intermediate protein CILP 1-1 showed a discrepancy with the literature as it was enriched in the deeper layers (LTP and MRM data in Supplementary Table S1 and S4a-e, respectively) and not in the intermediate zone (Lorenzo et al., 1998a). The other variant, CILP 1-2, was more evenly distributed in the MTP samples with the protein being somewhat more enriched in the intermediate zone. The reason for these differences is yet unknown but the current study involves tissue from a different joint, i.e. tibial knee cartilage versus femoral head cartilage (Lorenzo et al., 1998a). In support, a recent paper from our group shows that the molecular composition varies among different joints (Önnerfjord et al.,

**Table 2**

Regions of maximum protein abundance for superficial, intermediate and deep proteins. Depicted is the depth, in percentage of total tissue depth (from 0% = most superficial data point to 100% = deepest data point), at which a protein was found at maximum abundance (\*). Proteins with predominance in the superficial part showed maximum abundance in the uppermost 20% of the MTP samples, proteins with predominance in the intermediate part at 20%–35% of the tissue depth. Proteins with predominance in the deep part showed in general highest abundance in the lower 40% of the samples.

Superficial <sup>a)</sup>			Intermediate <sup>b)</sup>			Deep <sup>c)</sup>		
Protein	Sample	* (%)	Protein	Sample	* (%)	Protein	Sample	* (%)
Asporin	MTP36	18	Mimectan	MTP36	27	Aggrecan G1	MTP36	100
	MTP43	7		MTP43	30		MTP43	63
	MTP46	18		MTP46	35		MTP46	100
	MTP65	2		MTP65	20		MTP65	(38)
Tenascin-C	MTP36	18	Thrombospondin-1	MTP36	27	Chondroadherin	MTP36	92
	MTP43	7		MTP43	30		MTP43	80
	MTP46	18		MTP46	(18)		MTP46	100
	MTP65	7		MTP65	20		MTP65	100
Thrombospondin-4	MTP36	18	Link protein	MTP36	(51)	Osteoadherin	MTP36	92
	MTP43	7		MTP43	63		MTP43	63
	MTP46	10		MTP46	100		MTP46	100
	MTP65	2		MTP65	100		MTP65	100
Perlecan	MTP36	18				MTP36	92	
	MTP43	7				MTP43	63	
	MTP46	18				MTP46	100	
	MTP65	11				MTP65	100	

a) max. abundance within uppermost 20% of tissue depth.

b) max. abundance between 20% and 35% of tissue depth.

c) max. abundance within 60%–100% of tissue depth.

Parentheses indicate samples where the region of maximum protein abundance differs from the other samples.

2012). On the other hand, both the CILP 2 variants show more enrichment in the intermediate zone.

Most previous studies on protein distribution patterns were based on antibody-based technologies. Even though such studies can give a

detailed picture of protein localisation, they are often difficult to perform and interpret since they require specific antibodies and the accessibility of certain epitopes. The problem with epitope availability represents a common challenge when establishing immunohistochemistry

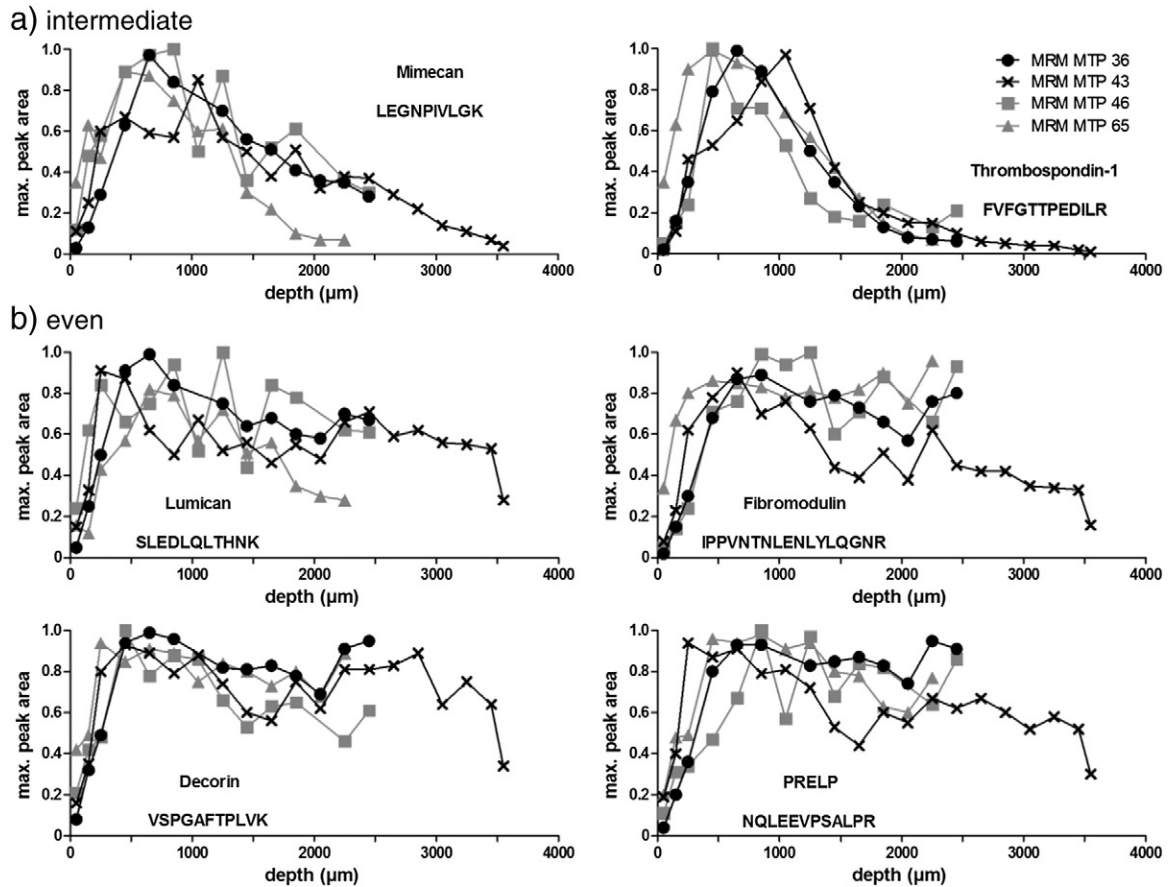
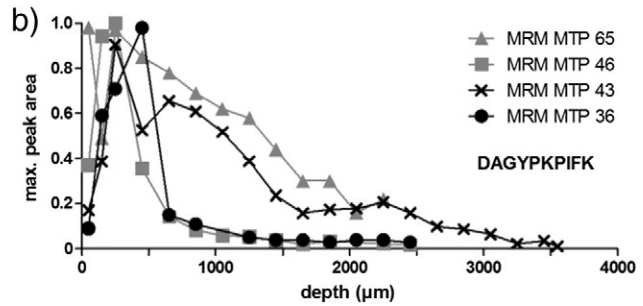
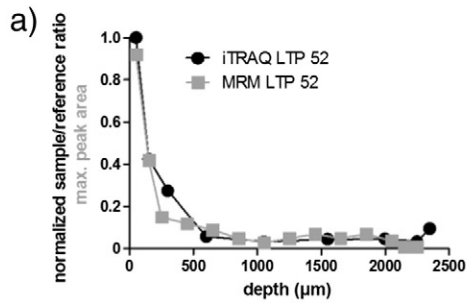
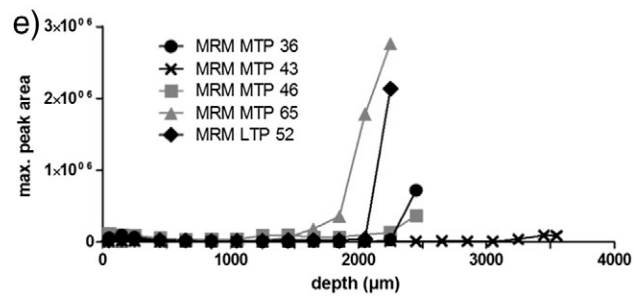
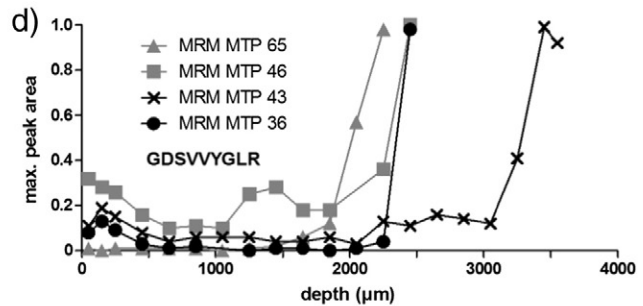
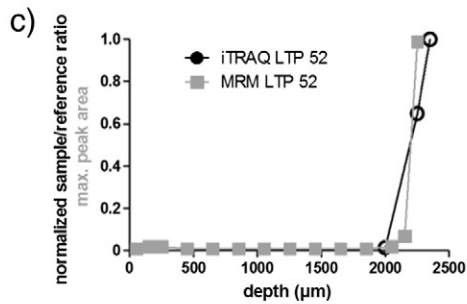


**Fig. 5.** Proteins enriched in the intermediate region or evenly distributed in the MTP samples. Proteins with a preferential distribution to the intermediate region (a) of the MTP samples or with an even distribution (b) throughout the tissue were quantified via MRM mass spectrometry. The peptide selected for the MRM assay is indicated for the respective protein. The MRM data were normalized to 1 by division of each data point with the highest one for a given peptide.

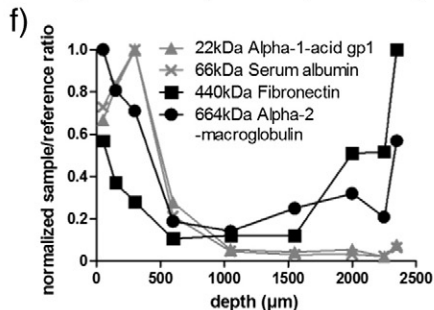
## Lubricin



## Osteopontin



## Serum proteins (LTP52, iTRAQ)



## Fibronectin (MTPs, MRM)

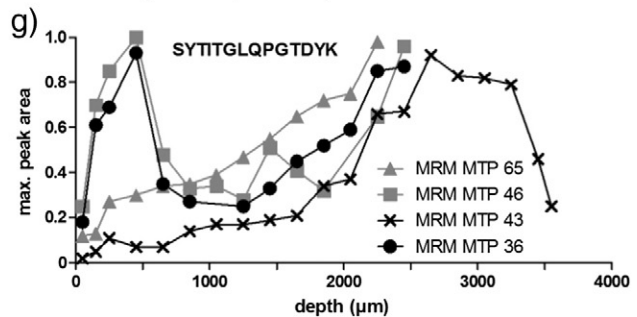


**Fig. 6.** Protein distribution patterns of lubricin, osteopontin and serum proteins. Lubricin was identified in the most superficial layers of the LTP52 by both the iTRAQ and MRM approach (a). Similarly, a predominance of lubricin in the superficial region was found in the four MTP samples using MRM (b). Osteopontin was identified in the deepest layers of the LTP52 by both iTRAQ and MRM (c). Similarly, a predominance of osteopontin in the deep region was found in the four MTP samples using MRM (d). Absolute values of osteopontin abundance by MRM showed a distinct increase of osteopontin content in the deepest layers in MTP36, 46, 65 and LTP52, but very low levels in MTP43 (e). Serum proteins analyzed in LTP52 showed different distribution patterns according to their molecular weight (f). The serum and ECM protein fibronectin showed heterogeneous distribution patterns in the four MTP samples (g). The peptide selected for the MRM assay is indicated for the respective protein. MRM and iTRAQ data in (a), (b), (c), (d), (f) and (g) were normalized to 1 by division of each data point with the highest one for a given peptide or peptide, respectively. MRM data in (e) shows absolute signal intensities. Open symbols in (c) indicate protein identification from one peptide only.

or immunofluorescence assays. Especially in cartilage, where there is a complex ECM with highly cross-linked macromolecules containing a multitude of different polysaccharide side chains, it is difficult to ensure efficient antibody penetration and epitope availability. This usually requires extensive antigen retrieval methods, e.g. incubation with proteolytic enzymes such as proteinase K or pepsin, incubation with enzymes to remove proteoglycan side chains such as chondroitinase ABC or heat-induced antigen retrieval using low or high pH buffer. There is a risk that these methods in themselves might alter the

molecular structure or even abolish the availability of certain epitopes. Furthermore, quantification of an antibody-based staining is challenging. Consequently, established antibody-based methods can give valuable information but require extensive optimization and quality control for each protein of interest. Mass spectrometry is regarded the state-of-the-art technique for protein identification, avoiding problems associated with antibody-based methods (Pecchini et al., 2012). Proteins are extracted and proteolytically digested to create peptides. These peptides are detected during mass spectrometry

and sophisticated methods for quantification have been established. Depending on the length of the proteins, several peptides identifying a certain protein are usually detected, thereby strengthening the identification.

It needs to be stressed, however, that protein analysis using mass spectrometry can only be performed on solubilized proteins. Covalently cross-linked proteins, like the fibrillar collagens except collagen type VI, are therefore not efficiently extracted. In a previous study, we investigated the extractability of selected ECM proteins (Önnerfjord et al., 2012). Aggrecan, asporin, chondroadherin and decorin showed an extractability of  $\geq 90\%$  from tibial knee cartilage, COMP of ca. 65% and lubricin of ca. 80%. An extraction efficiency of 100% cannot be reached due to the high degree of cross-linking of cartilage ECM molecules and thereby trapping of molecules in the matrix. Nevertheless, we think that conclusions about the relative distribution of proteins, comparing different zones with each other, can be made. Even though we detected chains of fibrillar collagens, e.g. collagen I alpha 1 and alpha 2 chains and collagen II alpha 1 chain (Supplementary Table S1) we chose not to draw any firm conclusions from these data since the extraction efficiency of, e.g. collagen II has been shown to be  $\leq 10\%$ . It is also unknown what this extractable pool represents, e.g. it could be newly synthesized collagen not incorporated into the matrix.

The MRM technology allows targeted quantitative proteomics with high sensitivity and accuracy (Gillette and Carr, 2013). Mass spectrometry and antibody-based methods might target different parts of a protein. Methodological differences might explain discrepancies between our study and previous reports. For example, we found collagen type VI at high levels in the superficial layers, while it has been reported from immunofluorescence studies to be located throughout the articular cartilage, possibly to a lesser extent in the superficial zone (Söder et al., 2002; Hansen et al., 2012; Wilusz et al., 2013). This discrepancy may be explained by the epitope not being exposed in the superficial zone, e.g. by interacting proteins masking the binding site. Although our results may reflect more efficient extraction from the superficial layers, most proteins discussed in this study (including collagen type VI) were found to be extractable in a previous study on full thickness knee cartilage (Önnerfjord et al., 2012). The observed distribution patterns of tenascin-C enriched in the superficial zone match previous immunohistochemical investigations (Veje et al., 2003). The identified patterns of distribution of several proteins match well with the gene expression investigated in the different zones of a human lateral femoral condyle in a study by Fukui et al. (2008). In this study, the genes of chondroadherin, CILP, link protein and aggrecan showed the highest expression in the deep cartilage region.

Articular cartilage is known to show inter- and intra-joint variability due to differences in mechanical load and architecture of the joints (Buckwalter and Mankin, 1998). Furthermore, even though articular cartilage zones are distinguished morphologically, the boundaries cannot be sharply defined. Therefore, it is difficult to compare structural studies with each other. In a quantitative study of the structural organization of human, medial femoral cartilage by Hunziker et al., the superficial zone was defined as the upper 10%, the transitional zone as the next 10% and the middle zone as the remaining 80% until the tidemark (Hunziker et al., 2002). When applying our approach as presented here to other areas in the knee as well as other joints, it will be possible to map structural differences and to define the different zones of articular cartilage in a more precise way. In the past, several studies focused on femoral condyle cartilage. We chose to analyze protein distribution patterns in tibial plateau cartilage since this area has the least curvature to its shape and therefore could be sectioned parallel to the joint surface in a reproducible manner. In future studies, it would be interesting to compare tibial and femoral cartilage of the opposing weight-bearing surfaces to each other. Furthermore, future studies will focus on understanding the functional importance of a distinct ECM composition in different

compartments, for example, by relating the molecular composition to biomechanical properties and cell distribution and metabolism.

This study provides a thus far unique overview of the ECM protein distribution in articular cartilage. This will have implications in basic research identifying structural-functional relations in cartilage ECM, as well as clinical approaches in tissue repair and design. In addition, comparing the protein distribution between healthy and pathological articular cartilage will give new insights into disease development and progression.

## 4. Experimental procedures

### 4.1. Materials

Filter tubes (molecular weight cut-off, 30 kDa) were purchased from PALL Life Sciences (Nanosep MI, USA). Reversed phase C18 (SUM-SS18V) spin columns were purchased from the Nest Group (MA, USA). Crude synthetic peptides were purchased from JPT (SpikeTides, JPT Peptide Technologies GmbH, Germany) and Thermo (Thermo-Fisher Scientific, Germany). A peptide mixture was made from the synthetic peptides (JPT) for checking system performance and retention times were adjusted using a peptide mixture (iRT Kit from Biognosys AG, Switzerland). Further reagents were described before (Önnerfjord et al., 2012).

### 4.2. Sample preparation

#### 4.2.1. Dissection, cryosectioning and extraction

Full-thickness macroscopically normal human articular cartilage from LTP and MTP were used in this study. The LTP sample was used to get an overview of the extractable proteins. The iTRAQ approach was used here to identify protein patterns and based on that, MRM assays for proteins of interest were established. Extracts from the same sample were then used to confirm the identification of similar protein patterns using the targeted and more sensitive MRM technology. The scarce availability of healthy human cartilage samples is a constant challenge in the field of cartilage research. For this reason, we chose to perform the initial feasibility test, method optimization and comparison between the two quantitative mass spectrometry approaches on the single LTP sample we obtained. MTP samples, more commonly associated with knee osteoarthritis (Felson et al., 2002), were then used to perform MRM analysis on four samples from the same joint region but from different individuals, thereby allowing identification of inter-individual variation.

The LTP sample was obtained from a 52-year-old male (LTP52) following amputation for bone tumours not involving the joint space (within 18 h of amputation) from the Stanmore Musculoskeletal BioBank following Research Ethics Committee approval (06/Q0506/31). The cartilage was rinsed briefly in PBS to remove traces of blood and synovial fluid and stored at  $-80\text{ }^{\circ}\text{C}$  until it was processed for experiments. Four MTP samples from forensic medicine cases from 36, 43, 46 and 65-year-old males with no previous joint disease history (MTP36, MTP43, MTP46, MTP65) were obtained from the University of Oslo, with approval by the local ethical committee (Önnerfjord et al., 2012). Full-depth cartilage plugs were cut into sections of  $10\text{ }\mu\text{m}$  thickness parallel to the cartilage surface starting from the superficial cartilage using a cryotome (chamber temperature,  $-18\text{ }^{\circ}\text{C}$ ; blade temperature,  $-21\text{ }^{\circ}\text{C}$ ). Ten consecutive sections were pooled. Sections were collected until a depth where accurate sectioning was no longer possible, presumably when reaching calcified tissue. Sample processing differed slightly between the LTP and the MTP samples due to optimization of the procedure (for detailed description of sample preparation, see Fig. 2). Initial experiments using Tissue Tek embedding of the tissue sample gave satisfactory results. These samples, however, had a tendency to clog the chromatographic system, most likely due to precipitation

of residual Tissue Tek components. These problems were avoided by removing Tissue Tek embedding from the protocol in later experiments.

It should be stressed that the focus of the study was to analyze protein distribution patterns within a certain specimen and then to compare these patterns in the different samples. This required constant section areas from top to bottom throughout a given sample, but made the different areas of the different samples irrelevant.

LTP52 sections were collected in the inner lid of an upside down-placed filter tube (0.45  $\mu\text{m}$  filter; Pall). Extraction was done for 24 h under gentle shaking at 4 °C in the lid of the filter tubes with 150  $\mu\text{l}$  of chaotropic extraction buffer (4 M guanidine hydrochloride, 50 mM sodium acetate, 100 mM 6-aminocaproic acid, 5 mM benzamidine, 5 mM *N*-ethylmaleimide; pH 5.8). The extract was obtained by centrifugation through the filter at 14000  $\times g$  for 3 min. Sections from the MTP samples were collected directly into centrifuge tubes and extracted as described above. Extracts were separated from extraction residues by centrifugation.

#### 4.2.2. Preparation for non-targeted quantitative mass spectrometry

In a discovery approach, the LTP52 sample was analyzed using the iTRAQ mass spectrometry approach (Ross et al., 2004). Reduction, alkylation and ethanol precipitation were performed as described before (Önnerfjord et al., 2012). Samples were suspended in 100  $\mu\text{l}$  0.1 mM triethylammonium bicarbonate buffer, pH 8.5, before trypsination with 1  $\mu\text{g}$  of trypsin at +37 °C on a shaker for about 16 h. The 24 depth fractions were collected into nine pools (Fig. 2). For this, equal sample amounts from the individual trypsin digests (one fraction representing the extract of 10 tissue sections representing a total depth of 100  $\mu\text{m}$ ) were mixed to achieve a volume of 20  $\mu\text{l}$ , thereby representing each sample fraction equally. To achieve a better resolution in the uppermost and lowest layers, the extracts of fraction 1, 2, 23 and 24 were not pooled with others. Three pools formed a sample set: set 1 (pools 1, 2 and 3), set 2 (pools 4, 5 and 6) and set 3 (pools 7, 8 and 9). With the iTRAQ technology, samples are labeled at the N-terminus with isobaric labels (label 114, 115 and 116), thereby giving the same mass adduct to all peptides, regardless of their origin. Labeled samples are mixed with a reference sample (label 117) as used in the study by Önnerfjord et al. (2012).

#### 4.2.3. Preparation for targeted mass spectrometry

Samples were digested with trypsin as described above, and aliquots of 10  $\mu\text{l}$  of the trypsin digest (from selected 100  $\mu\text{m}$  pools) were diluted to 200  $\mu\text{l}$  with 0.5 M ammonium bicarbonate and filtered through a 30 kDa filter. The high salt content was employed to minimize ionic interactions between positively charged tryptic peptides from ECM proteins and negatively charged glycosaminoglycans present in the sample. In brief, diluted digests were centrifuged at 2060  $\times g$  for 8 min through the filter followed by an additional wash with 100  $\mu\text{l}$  0.5 M ammonium bicarbonate. Before injection into the mass spectrometer, salts were removed from the filtrates using reversed-phase C18 spin columns according to the manufacturer's instructions.

#### 4.3. MRM assay generation

To generate protein-specific MRM assays, *in silico* trypsin digestion of proteins of interest was performed on 29 cartilage ECM proteins to identify proteotypic peptides for each protein (Fusaro et al., 2009). The following parameters were considered for peptide selection (i) unique peptides, (ii) peptides shorter than 20 amino acids, (iii) no missed cleavages, (iv) favoured  $\gamma$ -ions over  $\beta$ -ions, (v) favoured Q3 > Q1 and (vi) Q1/Q3 ratio between 400 and 1500  $m/z$  (Q1: peptide precursor ion mass, Q3: its specific fragment ion mass). We additionally used representative cartilage samples to select the final peptide list. Instrument parameters were then optimized for the highest sensitivity for all peptides and their transitions by using purchased crude synthetic peptides (JPT and Thermo). The measured peptide transitions are listed

in Supplementary Table S3. Three to six transitions for each peptide were measured in a scheduled MRM method.

#### 4.4. LC-MS setup and analysis

For the iTRAQ approach, the procedure was as previously described (Önnerfjord et al., 2012).

For the MRM samples, aliquots were injected and quantified using a TSQ Vantage triple quadrupole mass spectrometer (Thermo Scientific, Waltham MA) equipped with an Easy nano-LC system (Thermo Scientific, Waltham MA). The mass spectrometer was operated in MRM mode, with both Q1 and Q3 settings at 0.7 Da resolution. A spray voltage of +1700 V was used with a heated ion transfer setting of 270 °C for desolvation. Data were acquired using the Xcalibur software (version 2.1). Mobile phases used were A (0.1% formic acid in water) and B (0.1% formic acid in 100% acetonitrile). Separation was performed on 10  $\mu\text{m}$  tip; 75  $\mu\text{m}$   $\times$  15 cm capillary columns (PicoTip™ emitter; New Objective, Woburn, MA) packed with Reprosil-Pur C18-AQ resin (3  $\mu\text{m}$ , Dr. Maich GmbH). Samples were injected (2–4  $\mu\text{l}$ ) in duplicates, except for MTP46 due to technical reasons. The on-line reversed-phase separation was performed using a flow rate of 300 nl/min and a linear binary gradient from 3% B for 5 min to 15% B in 3 min, then to 35% B in 32 min and finally to 90% B in 3 min followed by a wash for 3 min with 90% B, and reconditioning to initial conditions in 10 min. A standard mixture of tryptic peptides was run to check the system performance of the LC-MS setup (Teleman et al., 2012).

#### 4.5. Data analysis

For the iTRAQ discovery approach, data analysis was done as previously described (Önnerfjord et al., 2012).

The targeted MRM data was analyzed using the Skyline 1.4 software (MacCoss Lab Software, University of Washington; MacLean et al., 2010). The relative signal from the individual transitions in combination with the expected retention time of the peak ensured the identity of the peak as measured by synthetic peptides during optimization. For simplicity reasons, the summed area of the individual transitions are presented in the selected figures throughout this paper.

We have used relative quantification in both approaches and not absolute values, i.e. the protein distribution patterns can be compared, but not the levels of different proteins. For clarity, values are presented normalized to 1 (maximum relative abundance) in the graphs.

The aggrecan core protein was analyzed individually for its three globular domains (G1, G2 and G3) to investigate differences in domain distribution with cartilage depth. Similarly, the cartilage intermediate layer proteins CILP 1 and CILP 2 were divided into their polypeptides CILP 1-1, 1-2, 2-1 and 2-2 for separate analysis (Lorenzo et al., 1998a; Lorenzo et al., 1998b; Johnson et al., 2003; Bernardo et al., 2011).

#### Author contributions

CM, AK, AA, DH and PÖ were involved in the conception and design of the study as well as the interpretation of the data. CM and AK conducted the experimental work. CM and AK made figures and tables and CM wrote the manuscript. CM, AK and PÖ conducted the mass spectrometry experiments and the data analysis. FR and JD provided forensic material and patient material, respectively. All authors critically revised the article, PÖ (corresponding author, E-mail: patrik.onnerfjord@med.lu.se) gave final approval of the article.

Supplementary data to this article can be found online at <http://dx.doi.org/10.1016/j.matbio.2014.08.013>.

#### Acknowledgements

This study was supported by the Swedish Research Council, King Gustaf V's 80-year fund, Greta & Johan Kock's, Alfred Österlund's and

Magnus Bergvall's foundations. The authors acknowledge the financial support by the European Union FP7-NMP-2008-LARGE, under contract no. 228929. We thank The Crafoord Foundation and the Inga-Britt & Arne Lundberg Foundation for funding the mass spectrometers used in this study. Catharina Müller was the recipient of a PhD stipend from the Faculty of Science, University of Copenhagen. We thank the National Institute of Health Research UK, for funding the procurement of tibial plateau cartilage sample used in this study (II-FS-0909-13007 to JD).

## References

- Ateshian, G.A., Soslowsky, L.J., Mow, V.C., 1991. Quantitation of articular surface topography and cartilage thickness in knee joints using stereophotogrammetry. *J. Biomech.* 24, 761–776.
- Bayliss, M.T., Venn, M., Maroudas, A., Ali, S.Y., 1983. Structure of proteoglycans from different layers of human articular cartilage. *Biochem. J.* 209, 387–400.
- Bernardo, B.C., Belluoccio, D., Rowley, L., Little, C.B., Hansen, U., Bateman, J.F., 2011. Cartilage intermediate layer protein 2 (CILP-2) is expressed in articular and meniscal cartilage and down-regulated in experimental osteoarthritis. *J. Biol. Chem.* 286, 37758–37767.
- Bhosale, A.M., Richardson, J.B., 2008. Articular cartilage: structure, injuries and review of management. *Br. Med. Bull.* 87, 77–95.
- Buckley, M.R., Bergou, A.J., Fouchard, J., Bonassar, L.J., Cohen, I., 2010. High-resolution spatial mapping of shear properties in cartilage. *J. Biomech.* 43, 796–800.
- Buckwalter, J.A., Mankin, H.J., 1998. Articular cartilage: tissue design and chondrocyte-matrix interactions. *Instr. Course Lect.* 47, 477–486.
- Cillero-Pastor, B., Eijkel, G.B., Kiss, A., Blanco, F.J., Heeren, R.M.A., 2013. Matrix-assisted laser desorption/ionization mass spectrometry: a new methodology to study human osteoarthritic cartilage. *Arthritis Rheum* 65, 710–720.
- DiCesare, P.E., Mörgelin, M., Carlson, C.S., Pasumarti, S., Paulsson, M., 1995. Cartilage oligomeric matrix protein: isolation and characterization from human articular cartilage. *J. Orthop. Res.* 13, 422–428.
- Felson, D.T., Nevitt, M.C., Zhang, Y., Aliabadi, P., Baumer, B., Gale, D., Li, W., Yu, W., Xu, L., 2002. High prevalence of lateral knee osteoarthritis in Beijing Chinese compared with Framingham Caucasian subjects. *Arthritis Rheum* 46, 1217–1222.
- Franzen, A., Heinegård, D., 1985. Isolation and characterization of two sialoproteins present only in bone calcified matrix. *Biochem. J.* 232, 715–724.
- Fukui, N., Miyamoto, Y., Nakajima, M., Ikeda, Y., Hikita, A., Furukawa, H., Mitomi, H., Tanaka, N., Katsuragawa, Y., Yamamoto, S., Sawabe, M., Juji, T., Mori, T., Suzuki, R., Ikegawa, S., 2008. Zonal gene expression of chondrocytes in osteoarthritic cartilage. *Arthritis Rheum.* 58, 3843–3853.
- Fusaro, V.A., Mani, D.R., Mesirov, J.P., Carr, S.A., 2009. Prediction of high-responder peptides for targeted protein assays by mass spectrometry. *Nat. Biotechnol.* 27, 190–198.
- Gillette, M.A., Carr, S.A., 2013. Quantitative analysis of peptides and proteins in biomedicine by targeted mass spectrometry. *Nat. Methods* 10, 28–34.
- Grogan, S.P., Duffy, S.F., Pauli, C., Koziol, J.A., Su, A.I., D'Lima, D.D., Lotz, M.K., 2013. Zone-specific gene expression patterns in articular cartilage. *Arthritis Rheum.* 65, 418–428.
- Guilak, F., Alexopoulos, L.G., Upton, M.L., Youn, I., Choi, J.B., Cao, L., Setton, L.A., Haider, M.A., 2006. The pericellular matrix as a transducer of biomechanical and biochemical signals in articular cartilage. *Ann. N. Y. Acad. Sci.* 1068, 498–512.
- Hansen, U., Allen, J.M., White, R., Moscibrocki, C., Bruckner, P., Bateman, J.F., Fitzgerald, J., 2012. WARP interacts with collagen VI-containing microfibrils in the pericellular matrix of human chondrocytes. *PLoS One* 7, e52793.
- Heinegård, D., 2009. Proteoglycans and more—from molecules to biology. *Int. J. Exp. Pathol.* 90, 575–586.
- Hoemann, C.D., Lafantaisie-Favreau, C.H., Lascau-Coman, V., Chen, G., Guzman-Morales, J., 2012. The cartilage–bone interface. *J. Knee Surg.* 25, 85–97.
- Hunziker, E.B., 2002. Articular cartilage repair: basic science and clinical progress. A review of the current status and prospects. *Osteoarthr. Cartil.* 10, 432–463.
- Hunziker, E.B., Quinn, T.M., Hauselmann, H.J., 2002. Quantitative structural organization of normal adult human articular cartilage. *Osteoarthr. Cartil.* 10, 564–572.
- Johnson, K., Farley, D., Hu, S.I., Terkeltaub, R., 2003. One of two chondrocyte-expressed isoforms of cartilage intermediate-layer protein functions as an insulin-like growth factor 1 antagonist. *Arthritis Rheum.* 48, 1302–1314.
- Kato, Y., Iwamoto, M., Koike, T., Suzuki, F., Takano, Y., 1988. Terminal differentiation and calcification in rabbit chondrocyte cultures grown in centrifuge tubes: regulation by transforming growth factor beta and serum factors. *Proc. Natl. Acad. Sci. U. S. A.* 85, 9552–9556.
- Li, G., Park, S.E., DeFrate, L.E., Schutzer, M.E., Ji, L., Gill, T.J., Rubash, H.E., 2005. The cartilage thickness distribution in the tibiofemoral joint and its correlation with cartilage-to-cartilage contact. *Clin. Biomech. (Bristol, Avon)* 20, 736–744.
- Lorenzo, P., Bayliss, M.T., Heinegård, D., 1998a. A novel cartilage protein (CILP) present in the mid-zone of human articular cartilage increases with age. *J. Biol. Chem.* 273, 23463–23468.
- Lorenzo, P., Neame, P., Sommarin, Y., Heinegård, D., 1998b. Cloning and deduced amino acid sequence of a novel cartilage protein (CILP) identifies a proform including a nucleotide pyrophosphohydrolase. *J. Biol. Chem.* 273, 23469–23475.
- MacLean, B., Tomazela, D.M., Shulman, N., Chambers, M., Finney, G.L., Frewen, B., Kern, R., Tabb, D.L., Liebler, D.C., MacCoss, M.J., 2010. Skyline: an open source document editor for creating and analyzing targeted proteomics experiments. *Bioinformatics* 26, 966–968.
- Mittelstaedt, D., Xia, Y., Shmelyov, A., Casciani, N., Bidthanapally, A., 2011. Quantitative determination of morphological and territorial structures of articular cartilage from both perpendicular and parallel sections by polarized light microscopy. *Connect. Tissue Res.* 52, 512–522.
- Mow, V.C., Ratcliffe, A., Poole, A.R., 1992. Cartilage and diarthrodial joints as paradigms for hierarchical materials and structures. *Biomaterials* 13, 67–97.
- Önnerfjord, P., Khabut, A., Reinholt, F.P., Svensson, O., Heinegård, D., 2012. Quantitative proteomic analysis of eight cartilaginous tissues reveals characteristic differences as well as similarities between subgroups. *J. Biol. Chem.* 287, 18913–18924.
- Pecchini, P., Malberti, F., Mieth, M., Quinn, R., Tripepi, G., Mallamaci, F., Maas, R., Zoccali, C., Ravani, P., 2012. Measuring asymmetric dimethylarginine (ADMA) in CKD: a comparison between enzyme-linked immunosorbent assay and liquid chromatography-electrospray tandem mass spectrometry. *J. Nephrol.* 25, 1016–1022.
- Pfister, B.E., Aydelotte, M.B., Burkhart, W., Kuettner, K.E., Schmid, T.M., 2001. Del1: a new protein in the superficial layer of articular cartilage. *Biochem. Biophys. Res. Commun.* 286, 268–273.
- Poole, A.R., Pidoux, I., Reiner, A., Rosenberg, L., 1982. An immunoelectron microscope study of the organization of proteoglycan monomer, link protein, and collagen in the matrix of articular cartilage. *J. Cell Biol.* 93, 921–937.
- Redler, I., Mow, V.C., Zimny, M.L., Mansell, J., 1975. The ultrastructure and biomechanical significance of the tidemark of articular cartilage. *Clin. Orthop. Relat. Res.* 357–362.
- Ross, P.L., Huang, Y.N., Marchese, J.N., Williamson, B., Parker, K., Hattan, S., Khainovski, N., Pillai, S., Dey, S., Daniels, S., Purkayastha, S., Juhasz, P., Martin, S., Bartlett-Jones, M., He, F., Jacobson, A., Pappin, D.J., 2004. Multiplexed protein quantitation in *Saccharomyces cerevisiae* using amine-reactive isobaric tagging reagents. *Mol. Cell. Proteomics* 3, 1154–1169.
- Schaefer, L., Schaefer, R.M., 2010. Proteoglycans: from structural compounds to signaling molecules. *Cell Tissue Res.* 339, 237–246.
- Schumacher, B.L., Block, J.A., Schmid, T.M., Aydelotte, M.B., Kuettner, K.E., 1994. A novel proteoglycan synthesized and secreted by chondrocytes of the superficial zone of articular cartilage. *Arch. Biochem. Biophys.* 311, 144–152.
- Schumacher, B.L., Su, J.L., Lindley, K.M., Kuettner, K.E., Cole, A.A., 2002. Horizontally oriented clusters of multiple chondrons in the superficial zone of ankle, but not knee articular cartilage. *Anat. Rec.* 266, 241–248.
- Shepherd, D.E., Seedhom, B.B., 1999. Thickness of human articular cartilage in joints of the lower limb. *Ann. Rheum. Dis.* 58, 27–34.
- Sodek, J., Ganss, B., McKee, M.D., 2000. Osteopontin. *Crit. Rev. Oral Biol. Med.* 11, 279–303.
- Söder, S., Hambach, L., Lissner, R., Kirchner, T., Aigner, T., 2002. Ultrastructural localization of type VI collagen in normal adult and osteoarthritic human articular cartilage. *Osteoarthr. Cartil.* 10, 464–470.
- Stockwell, R.A., Scott, J.E., 1967. Distribution of acid glycosaminoglycans in human articular cartilage. *Nature* 215, 1376–1378.
- Teleman, J., Karlsson, C., Waldemarson, S., Hansson, K., James, P., Malmstrom, J., Levander, F., 2012. Automated selected reaction monitoring software for accurate label-free protein quantification. *J. Proteome Res.* 11, 3766–3773.
- Veje, K., Hyllested-Winge, J.L., Ostergaard, K., 2003. Topographic and zonal distribution of tenascin in human articular cartilage from femoral heads: normal versus mild and severe osteoarthritis. *Osteoarthr. Cartil.* 11, 217–227.
- Wilusz, R.E., Zauscher, S., Guilak, F., 2013. Micromechanical mapping of early osteoarthritic changes in the pericellular matrix of human articular cartilage. *Osteoarthr. Cartil.* 21, 1895–1903.
- Youn, I., Choi, J.B., Cao, L., Setton, L.A., Guilak, F., 2006. Zonal variations in the three-dimensional morphology of the chondron measured in situ using confocal microscopy. *Osteoarthr. Cartil.* 14, 889–897.
- Zhang, Z., Jin, W., Beckett, J., Otto, T., Moed, B., 2011. A proteomic approach for identification and localization of the pericellular components of chondrocytes. *Histochem. Cell Biol.* 136, 153–162.